Ni^{3+}-Ni^{3+} pair transitions in highly doped $LiNbO_3$:Ni

M. G. Zhao
Institute of Solid State Physics, Sichuan Normal University, Chengdu 610068, People's Republic of China

G. G. Siu
Department of Physics, City Polytechnic of Hong Kong, Hong Kong
(Received 27 June 1994)

We report on the EPR Ni^{3+}-Ni^{3+} pair transitions in highly doped $LiNbO_3$:Ni. It is found that there are nine absorption peaks at 640, 1200, 1460, 1520, 3040, 3160, 3380, 7800, and 10 600 G in the range 0–12 000 G in highly doped $LiNbO_3$:Ni (0.8 wt. %). The spectra were interpreted as both the Ni^{3+} single-ion transitions and Ni^{3+}-Ni^{3+} pair transitions. In addition, it is found that many superhyperfine lines exist in the range 3000–3500 G which is not yet understood. Their origin is possibly an electron-phonon disturbance.

I. INTRODUCTION

The ferroelectric behavior and related properties in crystalline $LiNbO_3$ have been investigated in part by substituting a paramagnetic impurity such as Cu^{2+}, Cr^{3+}, Fe^{3+}, Mn^{2+}, or Ni^{2+} for a small fraction of the positive ions. The paramagnetic impurity ions, such as Fe^{3+}, then serve as a sensitive probe for investigating the crystalline environment and its response to ambient changes.[1] In studying the electron paramagnetic resonance (EPR) spectra of $LiNbO_3$:Cu^{2+}, $LiNbO_3$:Cr^{3+}, and YAG:Cr^{3+} where YAG is yttrium aluminum garnet, it is noticed that the low-field transition intensity increases with paramagnetic-impurity-ion doping and this has led to consideration of the interaction of neighboring Cu^{2+}, or Cr^{3+} ions by Zhao and Yan,[2] Zhao,[3] and Siu and Zhao.[4]

With a frequency-tunable EPR spectrometer Mirzakhanyan[5] identified the two possible $\Delta m_s = \pm 1$ transitions of Ni^{2+} signal ions in $LiNbO_3$:Ni. The splitting D was derived to be 152.1 ± 0.3 GHz and $g_{11} = 2.24 \pm 0.03$. Thiemann and Schirmer[6] have found that there is a $\Delta m_s = \pm 2$ transition of Ni^{2+} ions in $LiNbO_3$:Ni.

Here, we report EPR transitions observed at 9.553 GHz in $LiNbO_3$ doped with Ni (0.8 WT %). We will show that these transitions are induced by Ni^{2+} single ions, Ni^{3+} single ions, and the Ni^{3+}-Ni^{3+} pair.

II. MEASUREMENTS AND RESULTS

A single crystal of $LiNbO_3$:Ni(0.8 wt %) was grown by the Czochralski technique. The crystal axes were checked by x-ray analysis.

The EPR spectra were recorded on an x-band Brucker ER-200D spectrometer with 100 kHz field modulation. The spectra are shown in Figs. 1 and 2. Since D (=152 GHz) $\gg f$ (=9.553 GHz), the present spectra show no detectable signals of $\Delta m_s = \pm 1$ transitions of Ni^{2+} ions in the range 0–12 000 G. It can be seen from the figures that there are many resolved strong superhyperfine lines and nine absorption peaks at 640, 1200, 1460, 1620, 3040, 3160, 3380, 7800, and 10 600 G in the range 0–12 000 G in highly doped $LiNbO_3$:Ni. From the similarity between the EPR spectra of $LiNbO_3$:$Cr^{3+}(3d^3)$ with six-coordination C_3 symmetry[4] and the EPR spectra of $LiNbO_3$:Ni, we suggest that the absorption peaks are due to $Ni^{3+}(3d^7)$ with the ground state $^4A_1(F)$ which indicates that the impurity Ni^{3+} ions have the axially symmetric four-coordination (i.e., the 60^{2-}-20^{2-} vacancy) site rather than the six-coordination site. This is apparently to be expected in $LiNbO_3$, which generally has a rather imperfect crystal structure due to high doping.

III. INTERPRETATION OF EPR SPECTRA

With consideration of the exchange (or superexchange) interaction, the perturbation Hamiltonian for Ni^{3+}-ion pairs takes the form, for J much greater than the other terms,

$$\begin{aligned}\mathcal{H}_s &= \mathcal{H}_s(1)+\mathcal{H}_s(2)+J\mathbf{S}_1\cdot\mathbf{S}_2+DS_z^2 \\ &= g_z(1)\mu_B HS_z(1)+g_z(2)\mu_B HS_z(2)+D(1)S_Z^2(1) \\ &\quad +D(2)S_z^2(2)+J\mathbf{S}_1\cdot\mathbf{S}_2+DS_z^2 , \end{aligned} \tag{1}$$

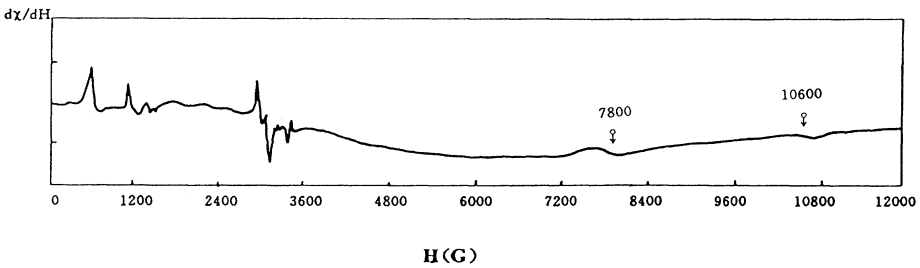

FIG. 1. EPR $d\chi/dH$ spectrum of a $LiNbO_3$:Ni crystal ($5\times5\times1.5$ mm^3). f=9.553 GHz; gain 2.5×10^4; test temperature, 77 K; $H//C_3$; ↬, pair transition.

0163-1829/95/51(10)/6246(3)/$06.00

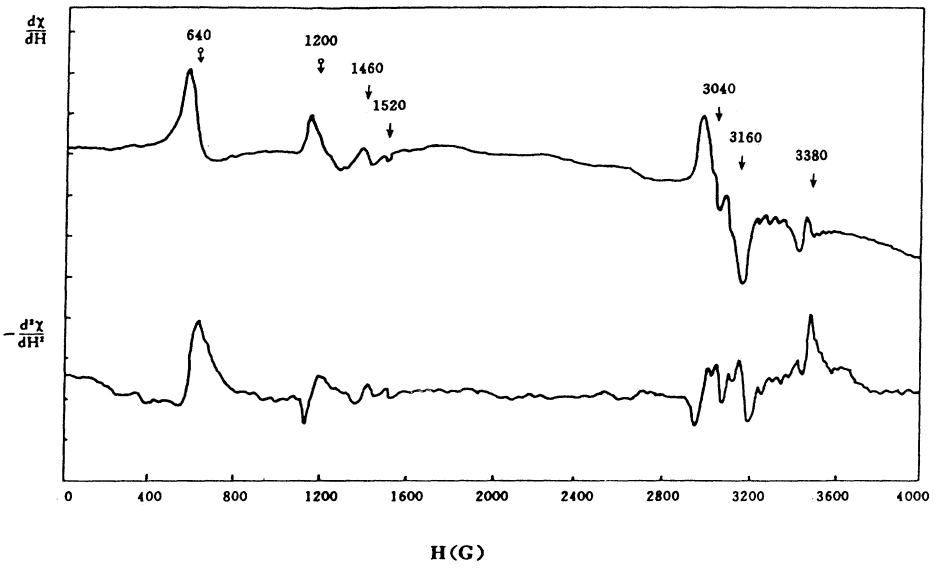

FIG. 2. EPR spectra of $LiNbO_3$: Ni crystal ($5\times5\times1.5$ mm^3). $f=9.553$ GHz; gain, 4×10^4 for $d\chi/dH$ (top spectrum), 2×10^5 for $-d^2\chi/dH^2$ (bottom spectrum); test temperature, 77 K; $H//C_3$; → single-ion transition; ⇢, pair transition. The upper part is the same as Fig. 1 on an expanded scale.

where H denotes the applied magnetic field, $\mathbf{S}=\mathbf{S}(1)+\mathbf{S}(2)$, $S(i)$ is the spin of the single ion $Ni^{3+}(i)$, $g_z(i)$ and $D(i)$ are the g factor and zero-field splitting parameter of the single ion $Ni^{3+}(i)$, respectively, and J is the exchange integral. D is the zero-field splitting parameter of the Ni^{3+}-Ni^{3+} pair which has a spin S due to the combination of the exchange (or superexchange) interaction, the magnetic dipole-dipole interaction, the spin-orbit coupling, and the low-symmetric crystal field, which can be expected to be different for the various values of S. $z\|C_3\|$ pair axis was used.

Since

$$\mathbf{S}_1\cdot\mathbf{S}_2=\tfrac{1}{2}[S(S+1)-S_1(S+1)-S_2(S_2+1)]\ ,$$

where S is the total effective spin of the final states of the two ions, the centers of gravity of the four spectroscopic states with $S=3$, 2, 1, and 0 are at energies $\frac{9}{4}J$, $-\frac{3}{4}J$, $-\frac{11}{4}J$, and $-\frac{15}{4}J$ at zero magnetic field, respectively; i.e., the largest term in Eq. (1), the exchange interaction, is diagonalized first. Resonance transitions are allowed only between states having the same total spin.

The resulting states are $|(\frac{3}{2},m_s';\frac{3}{2},m_s)S,Ms\rangle$ (the single-ion state symbols will be neglected in the coupled states). The resulting states are as follows:

$$\begin{aligned}
|3,3\rangle&=|\tfrac{3}{2},\tfrac{3}{2},\tfrac{3}{2},\tfrac{3}{2}\rangle\ ,\\
|3,2\rangle&=\frac{1}{\sqrt{2}}[|\tfrac{3}{2},\tfrac{3}{2};\tfrac{3}{2},\tfrac{1}{2}\rangle+|\tfrac{3}{2},\tfrac{1}{2};\tfrac{3}{2},\tfrac{3}{2}\rangle]\ ,\\
|3,1\rangle&=\frac{1}{\sqrt{5}}[|\tfrac{3}{2},\tfrac{3}{2};\tfrac{3}{2},-\tfrac{1}{2}\rangle+\sqrt{3}|\tfrac{3}{2},\tfrac{1}{2};\tfrac{3}{2},\tfrac{1}{2}\rangle\\
&\quad+|\tfrac{3}{2},-\tfrac{1}{2};\tfrac{3}{2},\tfrac{3}{2}\rangle]\ ,\\
|3,0\rangle&=\frac{1}{\sqrt{20}}[|\tfrac{3}{2},\tfrac{3}{2};\tfrac{3}{2},-\tfrac{3}{2}\rangle+3|\tfrac{3}{2},\tfrac{1}{2};\tfrac{3}{2},-\tfrac{1}{2}\rangle\\
&\quad+3|\tfrac{3}{2},-\tfrac{1}{2};\tfrac{3}{2},\tfrac{1}{2}\rangle-|\tfrac{3}{2},-\tfrac{3}{2};\tfrac{3}{2},\tfrac{3}{2}\rangle]\ ,
\end{aligned}\tag{2}$$

$$\begin{aligned}
|2,2\rangle&=\frac{1}{\sqrt{2}}[|\tfrac{3}{2},\tfrac{3}{2};\tfrac{3}{2},\tfrac{1}{2}\rangle-|\tfrac{3}{2},\tfrac{1}{2};\tfrac{3}{2},\tfrac{3}{2}\rangle]\ ,\\
|2,1\rangle&=\frac{1}{\sqrt{2}}[|\tfrac{3}{2},\tfrac{3}{2};\tfrac{3}{2},-\tfrac{1}{2}\rangle-|\tfrac{3}{2},-\tfrac{1}{2};\tfrac{3}{2},\tfrac{3}{2}\rangle]\ ,\\
|2,0\rangle&=\tfrac{1}{2}[|\tfrac{3}{2},\tfrac{1}{2};\tfrac{3}{2},-\tfrac{1}{2}\rangle+|\tfrac{3}{2},-\tfrac{3}{2};\tfrac{3}{2},\tfrac{3}{2}\rangle\\
&\quad-|\tfrac{3}{2},\tfrac{3}{2};\tfrac{3}{2},-\tfrac{3}{2}\rangle-|\tfrac{3}{2},-\tfrac{1}{2};\tfrac{3}{2},\tfrac{1}{2}\rangle]\ ,\\
|1,1\rangle&=\frac{1}{\sqrt{5}}[\sqrt{\tfrac{3}{2}}|\tfrac{3}{2},\tfrac{3}{2};\tfrac{3}{2},-\tfrac{1}{2}\rangle-\sqrt{2}|\tfrac{3}{2},\tfrac{1}{2};\tfrac{3}{2},\tfrac{1}{2}\rangle\\
&\quad+\sqrt{\tfrac{3}{2}}|\tfrac{3}{2},-\tfrac{1}{2};\tfrac{3}{2},\tfrac{3}{2}\rangle]\ ,\\
|1,0\rangle&=\frac{1}{\sqrt{20}}[3|\tfrac{3}{2},\tfrac{3}{2};\tfrac{3}{2},-\tfrac{3}{2}\rangle-|\tfrac{3}{2},\tfrac{1}{2};\tfrac{3}{2},-\tfrac{1}{2}\rangle\\
&\quad-|\tfrac{3}{2},-\tfrac{1}{2};\tfrac{3}{2},\tfrac{1}{2}\rangle+3|\tfrac{3}{2},-\tfrac{3}{2};\tfrac{3}{2},\tfrac{3}{2}\rangle]\ ,
\end{aligned}\tag{3}$$

$$\tag{4}$$

The expressions for the energy levels are as follows

(i) For single-ion transitions when $\Delta m_s=\pm1$,

$$\begin{aligned}
&-\tfrac{1}{2}\rightarrow\tfrac{1}{2}\text{:}\quad f=g_z\mu_BH\ ,\\
&-\tfrac{1}{2}\leftrightarrows-\tfrac{3}{2}\text{:}\quad f=\pm2D(i)\mp g_z(i)\mu_BH\ ,\\
&\tfrac{1}{2}\leftrightarrows\tfrac{3}{2}\text{:}\quad f=\pm2D(i)\pm g_z(i)\mu_BH\ ;
\end{aligned}\tag{5}$$

and when $\Delta m_s=\pm2$ (forbidden transitions),

$$-\tfrac{3}{2}\leftrightarrows\tfrac{1}{2},\quad f=\mp2D(i)\pm2g_z(i)\mu_BH\ .\tag{6}$$

(ii) For pair transitions with $\Delta Ms=\pm1$ and $S=1$,

$$\begin{aligned}
|1,0\rangle\rightarrow|1,1\rangle\text{:}\quad f&=\tfrac{1}{2}[g_z(1)+g_z(2)]\mu_\beta H+D\\
&\quad+\tfrac{3}{5}[D(1)+D(2)]\ ,\\
|1,1\rangle\rightarrow|1,0\rangle\text{:}\quad f&=-\tfrac{1}{2}[g_z(1)+g_z(2)]\mu_\beta H-D\\
&\quad-\tfrac{3}{5}[D(1)+D(2)]\ ,\\
|1,-1\rangle\rightarrow|1,1\rangle\text{:}\quad f&=[g_z(1)+g_z(2)]\mu_BH\ ;
\end{aligned}\tag{7}$$

with $S=2$,

TABLE I. Calculated and observed bands.

Single-ion transitions $g_z(1)=g_z(2)=2.019$, $D(1)=-170$ G, $D(2)=-110$ G		
$\lvert\frac{3}{2},m_s\rangle\rightarrow\lvert\frac{3}{2},M_s'\rangle$	H (G) (calc)	H (G) (obs)
$\lvert\frac{3}{2},-\frac{1}{2}\rangle\rightarrow\lvert\frac{3}{2},\frac{1}{2}\rangle$	3380; 3380	3380; 3380
$\lvert\frac{3}{2},-\frac{3}{2}\rangle\rightarrow\lvert\frac{3}{2},-\frac{1}{2}\rangle$	3040; 3160	3040; 3160
$\lvert\frac{3}{2},-\frac{3}{2}\rangle\rightarrow\lvert\frac{3}{2},\frac{1}{2}\rangle$	1520; 1580	1520; 1520
Pair transitions $D(S=1)=-3852$ G		
$\lvert1,M_s'\rangle\rightarrow\lvert1,Ms\rangle$	H (G) (calc)	H (G) (obs)
$\lvert1,0\rangle\rightarrow\lvert1,1\rangle$	7400	7800
$\lvert1,1\rangle\rightarrow\lvert1,0\rangle$	640	640
Pair transitions $D(S=2)=-4524$ G		
$\lvert2,M_s\rangle\rightarrow\lvert2,M_s'\rangle$	H (G) (Calc)	H (G) (obs)
$\lvert2,2\rangle\rightarrow\lvert2,1\rangle$	10 192	10 600
$\lvert2,0\rangle\rightarrow\lvert2,1\rangle$	3 380	3 380
Pair transitions $D(S=2)=D(S=3)=-4524$ G		
$\lvert3,M_s\rangle\rightarrow\lvert3,M_s'\rangle$	H (G) (calc)	H (G) (obs)
$\lvert3,1\rangle\rightarrow\lvert3,0\rangle$	1 200	1 200
$\lvert3,0\rangle\rightarrow\lvert3,1\rangle$	7 960	7 800
$\lvert3,2\rangle\rightarrow\lvert3,1\rangle$	10 360	10 600

$$
\begin{aligned}
&|2,1\rangle\rightarrow|2,2\rangle:\ f=\tfrac{1}{2}[g_z(1)+g_z(2)]\mu_\beta H+3D\ ,\\
&|2,2\rangle\rightarrow|2,1\rangle:\ f=-\tfrac{1}{2}[g_z(1)+g_z(2)]\mu_\beta H-3D\ ,\\
&|2,0\rangle\rightarrow|2,1\rangle:\ f=\tfrac{1}{2}[g_z(1)+g_z(2)]\mu_\beta H\ ;
\end{aligned}
\tag{8}
$$

and with $S=3$,

$$
\begin{aligned}
&|3,3\rangle\rightarrow|3,2\rangle:\ f=-\tfrac{1}{2}[g_z(1)+g_z(2)]\mu_\beta H-5D\\
&\qquad\qquad -[D(1)+D(2)]\ ,\\
&|3,1\rangle\rightarrow|3,0\rangle:\ f=-\tfrac{1}{2}[g_z(1)+g_z(2)]\mu_\beta H-D\\
&\qquad\qquad -\tfrac{1}{5}[D(1)+D(2)]\ ,\\
&|3,0\rangle\rightarrow|3,1\rangle:\ f=\tfrac{1}{2}[g_z(1)+g_z(2)]\mu_\beta H+D\\
&\qquad\qquad +\tfrac{1}{5}[D(1)+D(2)]\ ,
\end{aligned}
\tag{9}
$$

$$
\begin{aligned}
&|3,1\rangle\rightarrow|3,2\rangle:\ f=\tfrac{1}{2}[g_z(1)+g_z(2)]\mu_\beta H+3D\\
&\qquad\qquad +\tfrac{3}{5}[D(1)+D(2)]\ ,\\
&|3,2\rangle\rightarrow|3,1\rangle:\ f=-\tfrac{1}{2}[g_z(1)+g_z(2)]\mu_\beta H-3D\\
&\qquad\qquad -\tfrac{3}{5}[D(1)+D(2)]\ .
\end{aligned}
$$

Here f denotes the absorption frequency in the EPR measurement, $f=9.553$ GHz.

Both the calculated and experimental data are listed in Table I. It can be seen from Table I that the calculation is in good agreement with the experimental data.

IV. DISCUSSION AND CONCLUSIONS

(a) This work is a report on the Ni^{3+}-Ni^{3+} EPR pair transitions. It should be noted that, in contrast with the case of YAG:Cr^{3+},[3] the EPR lines at 3160, 3380, 7800, and 10 600 G extend below the zero signal level, although all other lines observed showed the typical phase of a derivative EPR absorption spectrum. This behavior of $LiNbO_3$:Ni^{3+} resonance is not yet understood. Possibly it is due to electron-phonon disturbances in the piezoelectric $LiNbO_3$.

(b) There exist many resolved strong superhyperfine lines in the range of 3000–3500 G. This is not yet understood because the nuclear spin I (^{58}Ni)=0. Possibly, it is again an electron-phonon disturbance in the piezoelectric $LiNbO_3$.

(c) The absorption intensity at 1460 G is larger than that at 1520 G. It is probably the $\Delta m_s=2$ transition of Ni^{2+}. According to the work by Müller,[7] Williams,[8] and Thiemann and Schirmer,[6] the $\Delta m_s=2$ transition is induced by the electric part of the microwave electric field.

(d) $LiNbO_3$ is a dielectric crystal that is of particular interest because of the photorefractive effect observed in these crystals. The photorefractive effect, which can be used for the storage of volume phase holograms, seems to be correlated to the presence of transition-metal impurities. For an understanding of the role of impurities in the photorefractive effect on a microscopic scale, it is necessary to know the valence state, and the sites of these impurities in the lattice. Therefore the discovery of both the Ni^{3+}-Ni^{3+} pair and four-fold-coordinated Ni^{3+} sites in the $LiNbO_3$ crystal seem to be significant findings.

(e) Models that have a correct and clear physical meaning will be those which agree well with experimental results. Therefore it is safe to say that the present model is reasonable.

ACKNOWLEDGMENTS

This work was supported by National Scientific Fund of China (Grant No. 1860897) and by the Committee of Education of Sichuan Province of China.

[1] M. G. Zhao and M. Chiu, Phys. Rev. B **49**, 12 556 (1994).
[2] M. G. Zhao and Q. L. Yang, Phys. Rev. B **39**, 862 (1989).
[3] M. G. Zhao, Phys. Rev. B **40**, 2543 (1989).
[4] G. G. Siu and M. G. Zhao, Phys. Rev. B **43**, 13 575 (1991).
[5] A. A. Mirzakhanyan, Sov. Phys. Solid State **23**, 1434 (1981).
[6] O. Thiemann and O. F. Schirmer, Phys. Status Solidi B **143**, K115 (1987).
[7] K. A. Muller, Phys. Rev. **171**, 350 (1968).
[8] F. I. B. Williams, Proc. Phys. Soc. London **91**, 111 (1967).